Optics Letters

Tunable holmium-doped fiber laser with multiwatt operation from 2025 nm to 2200 nm

Lars G. Holmen,[1,2,3,*] Peter C. Shardlow,[1] Pranabesh Barua,[1] Jayanta K. Sahu,[1] Nikita Simakov,[4] Alexander Hemming,[4] and W. Andrew Clarkson[1]

[1]Optoelectronics Research Centre, University of Southampton, Southampton, SO17 1BJ, UK
[2]Norwegian Defence Research Establishment (FFI), Kjeller, NO-2027, Norway
[3]Department of Technology Systems, University of Oslo, Kjeller, NO-2027, Norway
[4]Directed Energy Technologies and Effects, WCSD, Defence Science and Technology, Edinburgh, SA 5111, Australia
*Corresponding author: Lars. Holmen@ffi.no

Received 5 July 2019; revised 22 July 2019; accepted 23 July 2019; posted 23 July 2019 (Doc. ID 371776); published 21 August 2019

The emission band of holmium-doped silica fibers extends beyond 2200 nm, which means these lasers have the potential of covering considerable parts of the atmospheric transmission window between ~2100 nm and 2250 nm. However, efficient operation toward 2200 nm is challenging due to absorption in fused silica at the laser wavelength. Here we present a holmium-doped fiber laser specifically targeting long-wavelength operation. The laser is implemented as a high-feedback wavelength selective ring cavity and is tunable from 2025 nm to 2200 nm. A maximum slope efficiency of 58% is obtained at 2050 nm and a slope of 27% is obtained at 2200 nm. A power of 5.5 W from a single aperture (8.9 W total) is demonstrated at 2200 nm. Our results represent extended coverage of the 2 μm spectral band with multiwatt-level silica fiber lasers.

https://doi.org/10.1364/OL.44.004131

High power laser sources in the 2 μm spectral region are of great interest in a wide range of fields covering material processing, medicine, defense, and mid-IR generation through frequency conversion [1]. Lasers operating in the atmospheric transmission window between 2100 nm and 2250 nm are particularly attractive in applications involving free-space beam propagation such as lidar and remote sensing, free-space communications, and directed energy systems. Eye safety is an additional vital consideration in such applications, and 2 μm emission is strongly preferred over more conventional 1 μm sources.

Both thulium- and holmium-doped silica fiber lasers emit in the 2 μm band. Thulium fiber lasers provide excellent performance around 2 μm, but efficient operation above ~2100 nm is challenging [2,3]. Operation of thulium lasers at 2198 nm has been demonstrated using a high feedback cavity, with reports of slope efficiencies of 17% and modest power levels of 550 mW [4]. In comparison, Ho lasers provide extended coverage into the atmospheric transmission window due to a slightly redshifted emission peak that reduces issues with parasitic operation when tuned to longer wavelengths. For instance, high power operation of a Ho fiber laser tunable from 2040 nm to 2170 nm with reasonable efficiency has previously been demonstrated [5].

Ultimately, the limiting factor for long-wavelength operation of rare-earth-doped fiber lasers is the diminishing emission cross section and competition from gain in the "natural" operating region, leading to dominating amounts of amplified spontaneous emission (ASE) and parasitic lasing. Different strategies have been explored to facilitate laser emission at longer wavelengths. First, filtering techniques can be used, where additional losses are introduced at short wavelengths. This can be achieved by using, e.g., photonic band gap technology [6], or by heating the quasi-three-level gain medium to enhance reabsorption [7]. Second, inversion management has been shown to provide extended operation by limiting the gain at short wavelengths. By pumping resonantly at long wavelengths, the excitation can be distributed over a long fiber, whereby the gain spectrum is redshifted since the maximum inversion is lowered [7,8]. Finally, long-wavelength operation can be achieved using high Q cavities with selective feedback to obtain sufficient gain, although this is inevitably associated with reduced efficiency.

Operation of holmium silica fiber lasers toward 2.2 μm presents challenges due to the reduced emission cross section but also increasing propagation losses associated with the multiphonon absorption edge of the host material. Another major source of loss in this spectral regime is caused by the $\nu_3 + \nu_1$ vibrational combination mode of bound hydroxyl (SiOH) [9]. Loss from OH^- contamination can be significant in the entire 2 μm band but is particularly detrimental around 2.2 μm where the absorption peaks. This puts stringent requirements on fiber fabrication to minimize OH^- inclusion, and concentrations below the ppm level are essential [5]. The propagation losses exclude the approach of inversion management by increasing the fiber length and pumping in-band at long wavelengths [7]. Instead of gain suppression at short wavelengths, high feedback with strong wavelength selectivity becomes necessary for stable long-wavelength operation. Previous studies have shown Ho fiber lasers operating out to 2210 nm [10]; however, an extremely high Q-cavity configuration with highly

reflective fiber Bragg gratings on both ends was required for suppressing shorter wavelength parasitic lasing. This limited the slope efficiency to 4% and the power to 140 mW.

In this Letter, we investigate the limits of long-wavelength tuning of a holmium-doped fiber laser and report for the first time, to the best of our knowledge, watt-level output from a silica fiber laser operating beyond 2.2 μm. A tunable ring oscillator was built and optimized for long-wavelength operation, where the ring cavity avoids double-pass ASE and reduces propagation losses through single-pass amplification. High wavelength selective feedback from a transmission diffraction grating allowed continuous tuning and stable laser operation from 2025 nm to 2200 nm, with a maximum output power of 22.7 W obtained at 2100 nm and 8.9 W at 2200 nm. With a laser slope efficiency of 27% demonstrated at 2200 nm, considerable power scaling of fiber laser sources in this spectral regime is seen to be viable.

The laser setup is illustrated in Fig. 1. Light from a Tm-doped fiber laser was free-space launched through a dichroic mirror into the core of a 6.5 m long Ho-doped fiber (core diameter 14 μm, numerical aperture 0.12). The Tm pump laser was cladding-pumped with a 790 nm diode laser and was capable of delivering > 60 W from a single-mode fiber. A fiber Bragg grating locked the pump wavelength to 1958 nm, and the laser had a linewidth below 0.1 nm. The inhouse fabricated Ho fiber had a small signal absorption of 35 dB/m at 1950 nm and extremely low levels of OH^- contamination below 0.1 ppm both in the core and the cladding [11]. The fiber had an all-glass triple clad design suitable for resonant 2 μm cladding pumping, in which configuration slope efficiencies of up to 70% with respect to absorbed pump power have been demonstrated [11]. The pure silica inner cladding of this fiber had a 65 μm octagonal cladding (flat-to-flat), which was overjacketed with 180 μm of low-index fluorine-doped silica.

Both ends of the gain fiber were CO_2-laser-bonded to antireflection-coated (AR) end caps to suppress broadband feedback and parasitic lasing. An intracavity fused silica transmission grating (560 lines/mm) in a Littrow configuration provided wavelength selective feedback with the first diffracted order fed into the other end of the fiber to form a tunable ring cavity. The angular dispersion introduced by the grating was converted to a spatial chirp of wavelengths in the focal plane of lens L2. Tuning was achieved by translating the fiber end in this plane, as indicated by the arrow in Fig. 1. For large wavelength shifts, L2 was also translated to avoid coupling losses from off-axis beam propagation. The lenses used were Infrasil triplets with a 25 mm focal length and were positioned to obtain a collimated beam in the tuning cavity with a measured $D4\sigma$ beam diameter of 4.4 mm. Outcoupling was achieved with mirror M1, which had a reflectance of 20% on one side and an AR-coating on the other. Unidirectional operation was forced by retroreflecting the reverse output arm from M1 [12,13], and the fraction of light circulating in the wrong direction was determined from the power transmitted through M2 ($R = 60\%$). Unabsorbed pump light is for clarity not shown in the schematic but was measured on a separate power meter. Optical spectra were measured with an optical spectrum analyzer (Yokogawa AQ6375); a pyroelectric array (Spiricon Pyrocam III) was used for beam imaging; and a scanning slit beam profiler (Ophir NanoScan 2s Pyro) was used for measuring the M^2 beam quality.

Figure 2 shows the maximum output power when tuning from 2025 nm to 2200 nm for a pump laser power of 42 W. The highest power of 22.7 W was obtained at 2100 nm, whereas 8.9 W was output at 2200 nm. A core launch efficiency between 80% and 90% was estimated from measurements of small signal absorption; however, light not coupled into the core is still guided by the all-glass cladding and is partially absorbed. Despite the fiber having an all-glass cladding, core pumping was chosen in this work since it improved long-wavelength performance by reducing the fiber length and propagation losses. For operation toward the edge of the tuning range, parasitic lasing at shorter wavelengths (2050 nm to 2080 nm) indicative of nonsaturable gain appeared when the absorbed pump powers exceeded ~40 W and prevented further power scaling at 2200 nm.

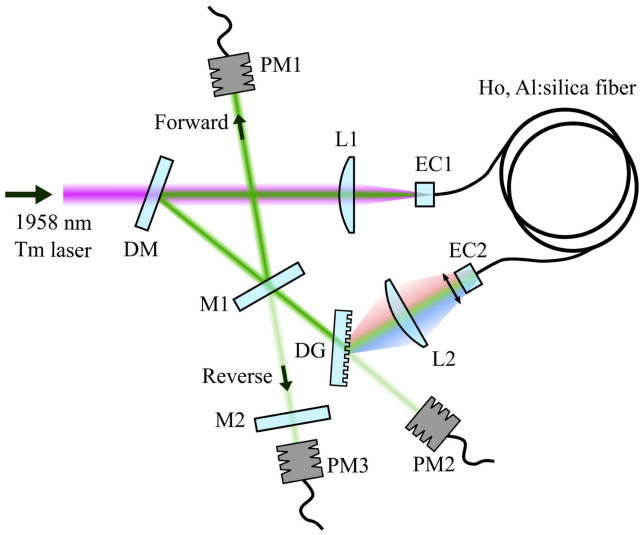

Fig. 1. Schematic of the tunable Ho-doped fiber laser, containing a dichroic mirror (DM), mirrors (M), a diffraction grating (DG), power meters (PM), end caps (EC), and lenses (L). The laser oscillates in the counterclockwise direction.

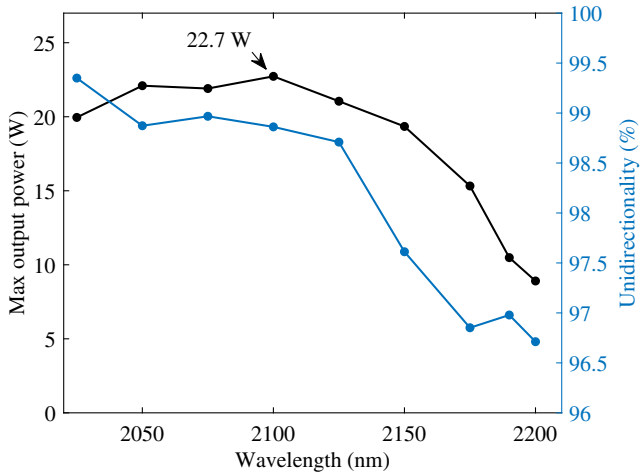

Fig. 2. Maximum output power (black) and the degree of unidirectionality (blue) measured at different wavelengths. The pump laser power was 42 W.

The reflected signal from M2 in Fig. 1 serves as an injected signal for the counterclockwise (CCW) oscillating light, such that the presence of any clockwise (CW) light causes growth of the CCW oscillation [p. 535, 12]. Figure 2 shows the degree of unidirectionality measured over the tuning range. Although full extinction of CW light was not achieved using this technique, laser operation with >96% of the light circulating CCW was seen over the whole tuning range. The unidirectionality was observed to decrease with wavelength from 99.4% at 2025 nm to 96.7% at 2200 nm for unknown reasons that were not further investigated. Notably, unidirectional operation was achieved without the use of a Faraday isolator, which was desirable both due to the limited availability of high power isolators in this spectral regime and because the inclusion of an isolator would add a considerable intracavity loss, which is particularly undesirable in this high feedback cavity.

Normalized optical spectra from operating the laser at wavelengths between 2025 nm and 2200 nm in steps of 25 nm are shown in Fig. 3. Tuning was limited on the short wavelength side by increasing transmission in the dichroic mirror used for pump coupling and at long wavelengths by parasitic lasing. Excellent spectral quality is observed across the tuning range, although some short-wavelength ASE is observed when lasing at 2200 nm. The optical signal-to-noise ratio at this wavelength was 45 dB (2 nm spectral resolution), and the in-band power content was measured to >99.8%.

A detailed optical spectrum for operation at 2200 nm is shown in Fig. 4. Although this particular spectrum is narrow with a full width at half-maximum linewidth of 0.17 nm, the linewidth was observed to vary slightly with pump power but did not exceed ~0.5 nm. Figure 4 also shows the beam profile of the collimated beam at the output from mirror M1, where some beam deformation is observed despite the gain fiber being robustly a single mode at this wavelength. This is attributed to the presence of small amounts of cladding light, which was confirmed by imaging the fiber end face. The high feedback cavity design made the beam profile sensitive to the intracavity core-to-core coupling, since light not launched into the core was guided by the all-glass cladding. The M^2 beam quality was measured to vary between 1.2 and 1.4.

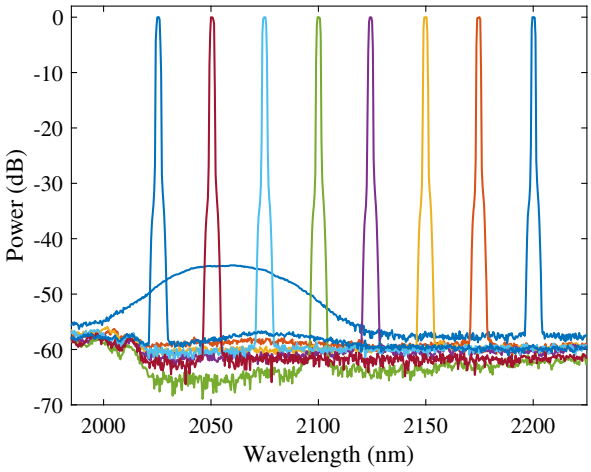

Fig. 3. Normalized optical spectra (2 nm resolution).

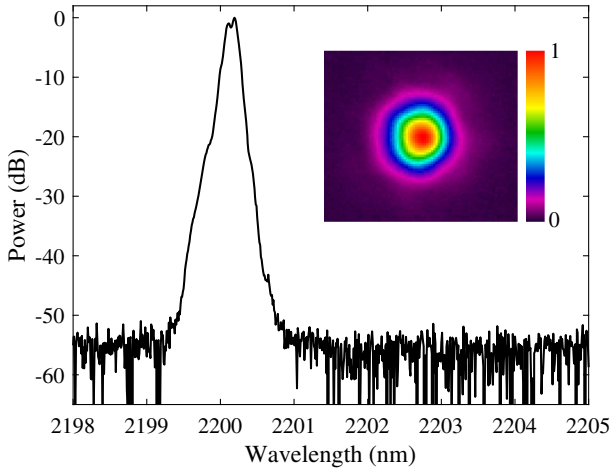

Fig. 4. Optical spectrum at 2200 nm measured with a 0.05 nm resolution. The inset shows the beam profile.

Figure 5 shows the power curve recorded when operating the laser at 2200 nm. The transmission grating used in the tuning cavity had a diffraction efficiency into the 1st order of ~95% for *s*-polarization, but only ~30% for *p*-polarization. When combined with depolarization that occurred due to the random birefringence of the fiber, this led to a considerable amount of power lost from the cavity through the zeroth order of the diffraction grating. This fraction was found to vary with power and depend on the fiber coiling. For the power curve in Fig. 5, 5.5 W was measured from the outcoupling mirror out of a total power of 8.9 W.

Active polarization control was not implemented in this work. By twisting and coiling the fiber, the power reflected from the output coupler and the power leaking through the grating were observed to be anticorrelated, and the power fraction exiting the output coupler could manually be improved to nearly 90%. However, this was only the case for a specific operating point, and it was not possible to optimize fiber

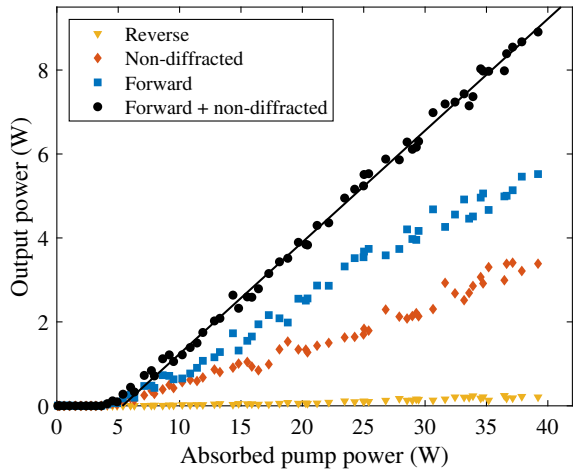

Fig. 5. Power curve measured at 2200 nm, showing the combined and separate contributions of forward power from the output coupler (PM1 in Fig. 1) and nondiffracted light leaking through the grating (PM2). The laser power circulating in the reverse direction as measured with PM3 is also shown.

birefringence through twisting and coiling to achieve a predominantly linear polarization at all pump powers. Therefore, the fiber was left loosely coiled, and the total power obtained from adding the two output arms is used to evaluate intrinsic laser performance.

The slope efficiency at 2200 nm for the total laser output in Fig. 5 was 27%. This was measured with respect to the absorbed pump power, because thermal lensing in the coupling optics caused a power dependent core launch efficiency and hence a nonlinear power curve with respect to launched power. Alignment was optimized at maximum power, where a pump absorption of 93% was obtained. The pump absorption was higher for operation at shorter wavelengths where pump saturation was less significant. Figure 6 shows the slope efficiency and threshold from power curves at the different wavelengths. A slope above 55% was obtained at the optimum part of the tuning range between 2050 nm and 2125 nm. This is lower by 10% to 20% compared to experiments with the same fiber in linear cavities with high output coupling [11]. This is attributed to intracavity coupling losses combined with the increased impact of core propagation loss in a high feedback resonator.

It was confirmed that higher outcoupling ratios could be used for increasing efficiency in the parts of the tuning range closer to the peak gain, but the high wavelength-selective feedback was found necessary for stable 2200 nm operation. A selection of different output coupling mirrors were tested in the laser, and the mirror that provided the highest possible outcoupling while maintaining good spectral quality out to 2200 nm was chosen. The effective feedback to the laser in the current configuration is estimated to 50% by considering the output coupling from the mirror M1 (20%) and the fraction of non-diffracted light (13%, estimated from Fig. 5), and assuming a realistic core-to-core coupling efficiency of 80%.

The slope efficiency was nearly constant at ∼55% up to a wavelength of 2125 nm, beyond which it drops monotonically toward 27% at 2200 nm. Still, even at 2200 nm a reasonable slope efficiency close to 30% is achieved, which means that power scaling in the 2150 nm to 2200 nm spectral region is viable. Further improvements of power and efficiency are expected from optimizing the resonator design, for instance a fixed wavelength all-fiber laser with fiber Bragg gratings.

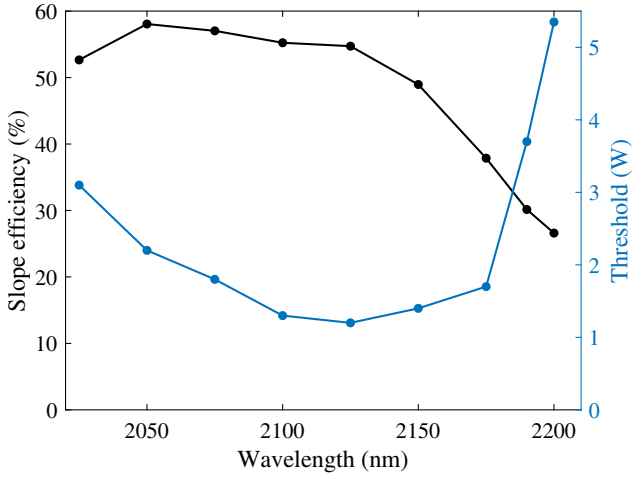

Fig. 6. Slope efficiency (black) and threshold (blue) of the laser across the tuning range, both measured with respect to absorbed pump power.

In conclusion, we have presented a tunable holmium-doped fiber laser targeting long-wavelength operation and for the first time demonstrated watt-level power from a silica fiber laser operating at 2200 nm. Using a high-feedback ring laser with an inhouse-developed holmium gain fiber with low OH^- contamination, stable and continuously tunable operation with excellent spectral quality was obtained from 2025 nm to 2200 nm. Unidirectional operation of the ring laser with a contrast better than 25:1 was achieved without the use of a Faraday isolator by retroreflecting one of the laser output arms. The laser operated with a slope efficiency with respect to absorbed power of 58% at 2050 nm and 27% at 2200 nm, and delivered an output power of 5.5 W from a single aperture (8.9 W total) at 2200 nm. Although propagation losses at the infrared absorption edge of fused silica reduces the efficiency toward 2200 nm, these results suggest that power scaling to the multitens of watt regime from a single aperture should be possible with the use of improved cavity configurations with reduced intracavity losses. To the best of our knowledge, these results represent the highest power from silica fiber lasers operating beyond 2170 nm reported in the published literature, extending the coverage of the 2100 nm to 2250 nm atmospheric transmission window with high power fiber lasers.

Funding. Seventh Framework Programme (287732).

Acknowledgment. The authors thank Stig E. Landrø (FFI) for input on coupling optics. Portions of this work were presented at CLEO/Europe 2019, paper CJ-8.6. The data for this work is accessible through the University of Southampton Institutional Research Repository (https://doi.org/10.5258/SOTON/D0987).

REFERENCES

1. A. Hemming, N. Simakov, J. Haub, and A. Carter, Opt. Fiber Technol. **20**, 621 (2014).
2. A. Sincore, J. D. Bradford, J. Cook, L. Shah, and M. C. Richardson, IEEE J. Sel. Top. Quantum Electron. **24**, 0901808 (2018).
3. F. Liu, P. Liu, X. Feng, C. Wang, Z. Yan, and Z. Zhang, Opt. Express **27**, 8283 (2019).
4. J. Li, Z. Sun, H. Luo, Z. Yan, K. Zhou, Y. Liu, and L. Zhang, Opt. Express **22**, 5387 (2014).
5. N. Simakov, A. Hemming, W. A. Clarkson, J. Haub, and A. Carter, Opt. Express **21**, 28415 (2013).
6. A. Shirakawa, M. Chen, K. I. Ueda, C. B. Olausson, J. K. Lyngsø, and J. Broeng, Opt. Fiber Technol. **16**, 449 (2010).
7. M. P. Kalita, S.-U. Alam, C. Codemard, S. Yoo, A. J. Boyland, M. Ibsen, and J. K. Sahu, Opt. Express **18**, 5920 (2010).
8. N. Simakov, Z. Li, Y. Jung, J. M. O. Daniel, P. Barua, P. C. Shardlow, S. Liang, J. K. Sahu, A. Hemming, W. A. Clarkson, S.-U. Alam, and D. J. Richardson, Opt. Express **24**, 13946 (2016).
9. O. Humbach, H. Fabian, U. Grzesik, U. Haken, and W. Heitmann, J. Non-Cryst. Solids **203**, 19 (1996).
10. S. O. Antipov, V. A. Kamynin, O. I. Medvedkov, A. V. Marakulin, L. A. Minashina, A. S. Kurkov, and A. V. Baranikov, Quantum Electron. **43**, 603 (2013).
11. P. C. Shardlow, N. Simakov, A. Billaud, J. M. O. Daniel, P. Barua, J. K. Sahu, A. Hemming, and W. A. Clarkson, *Conference on Lasers and Electro-Optics Europe & European Quantum Electronics Conference (CLEO/Europe-EQEC)* (2017), pp. CJ–11–4.
12. A. Siegman, *Lasers* (University Science Books, 1986).
13. M. Hercher, M. Young, and C. B. Smoyer, J. Appl. Phys. **36**, 3351 (1965).